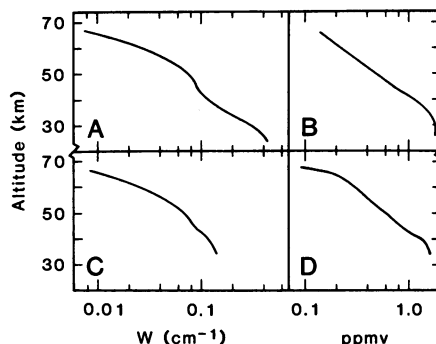


Fig. 2. (A) Equivalent width,  $W$ , of the absorption feature at  $3017.8\text{ cm}^{-1}$  as a function of tangent altitude of the line of sight to the sun center. (B) Inverted  $\text{CH}_4$  volume mixing ratio computed on the basis of the U.S. standard atmosphere (1966) for the atmospheric temperature and total number density profile versus altitude. (C) Equivalent width of the  $2979\text{-cm}^{-1}$   $\text{CH}_4$  manifold versus tangent altitude. (D) Deduced  $\text{CH}_4$  vertical distribution (ppmv, parts per million by volume).



to  $30^\circ$ . The sunrise observations took place at high southern latitudes and provided pertinent information on inter-hemispheric seasonal variations of the observed atmospheric species, such as atmospheric CO.

In addition to solar infrared absorption features, many of which had not been observed before, atmospheric spectral absorptions due to CO and  $\text{CO}_2$  were observed at heights ( $H$ ) tangent to the thermosphere ( $H > 85\text{ km}$ ); absorptions due to  $\text{O}_3$ ,  $\text{H}_2\text{O}$ ,  $\text{CH}_4$ , and  $\text{N}_2\text{O}$  were observed in the mesosphere ( $H > 50\text{ km}$ ); and the strongly coupled molecules NO- $\text{NO}_2$  and HCl-HF were simultaneously observed in the same stratospheric regions. In this report we present the first results on methane in the mesosphere, where it had not been measured before.

Since its only atmospheric source is at ground level, methane has been used by atmospheric modelers as a vertical transport indicator. Its increasingly efficient oxidation at higher altitudes in the stratosphere leads to a continuous reduction of its volume concentration with altitude. Methane absorptions were observed from Spacelab in three sunset runs at two different spectral intervals in the  $3.3\text{-}\mu\text{m}$   $\nu_3$  fundamental band. A spectrum of most of its  $Q$  branch, recorded in 2 seconds while the line of sight to the sun center grazed an altitude of  $26\text{ km}$  above the geoid, is shown in Fig. 1A. Figure 1B shows a synthetic spectrum of the same spectral region computed with the results of the inversion of the measured absorptions.

Figure 2A shows the measured equivalent width of the absorption feature at  $3017.8\text{ cm}^{-1}$ . It is essentially due to five absorption lines, whose parameters (5) have been used to deduce the vertical distribution shown in Fig. 2B. This result was verified with synthetic spectra of the whole region except below  $\sim 30\text{ km}$ , where slightly lower values are obtained; this discrepancy could originate from the saturation of these lines at very low altitudes. Figure 2C shows the equivalent

width of the  $\text{CH}_4$  manifold centered at  $2979\text{ cm}^{-1}$  as a function of altitude, and Fig. 2D shows the corresponding inverted data and allows a comparison of the volume concentration profiles in two wavelength ranges.

These measurements at low latitudes agree with data (6) reported for the  $25^\circ$  to  $35^\circ$  latitude band in the stratosphere. At higher altitudes, where chemical oxidation processes become less efficient, another destruction process is needed to explain the mesospheric concentration decrease with altitude. Photodissocia-

tion of  $\text{CH}_4$  in particular by solar Lyman- $\alpha$  radiation, plays a dominant role in modeling for higher altitudes.

M.-P. LEMAITRE, J. LAURENT  
J. BESSON, A. GIRARD

Office National d'Etudes  
et de Recherches Aérospatiales,  
F-92320 Châtillon, France

C. LIPPENS, C. MULLER  
J. VERCHEVAL, M. ACKERMAN  
Belgian Institute for Space Aeronomy,  
B-1180 Brussels, Belgium

#### References and Notes

1. M. Ackerman, in *Atmospheric Physics from Spacelab*, J. J. Burger, A. Pedersen, B. Battick, Eds. (Reidel, Dordrecht, Netherlands, 1976), pp. 107-116.
2. A. Girard and P. Jacquinet, in *Advanced Optical Techniques*, A. C. S. Van Heel, Ed. (North-Holland, Amsterdam, 1967), pp. 73-121.
3. A. Girard, *Appl. Opt.* **2**, 79 (1963).
4. J. Laurent, M.-P. Lemaître, C. Lippens, C. Muller, *Aeronaut. Astronaut.* **98**, 60 (1983).
5. L. S. Rothman *et al.*, *Appl. Opt.* **22**, 2247 (1983).
6. *The Stratosphere 1981, Theory and Measurements* (NASA-Goddard Space Flight Center, Greenbelt, Md., 1982), pp. 1-37.
7. We wish to acknowledge the support of the Belgian Ministries of Education and of Science Policy, the French Centre National d'Etudes Spatiales, and the French Ministry of Research and Industry.

27 March 1984; accepted 10 May 1984

## Waves in the OH Emissive Layer

**Abstract.** An instrument designed to take pictures of infrared spatial structures from space was flown on Spacelab 1. An image intensifier was used to give enough sensitivity and images were recorded on photographic film. The instrument worked perfectly and 1771 pictures were obtained during the night on 27 orbits (one picture every 16 seconds). Image processing of the data will yield information about the extension of large-scale structures and the relation between medium-scale structures and gravity waves.

It was recently discovered that the night sky exhibits patchy structures (1-3). This surprising result was obtained by taking pictures during dark moon periods with a fast lens and infrared photographic emulsion. Figure 1 is an example of such a display. Triangulation measure-

ments give an altitude of  $85\text{ km}$  for these structures, which are luminous by themselves. They look similar to noctilucent clouds, which are illuminated by the sun; however, the infrared structures can be seen at a solar depression angle of  $-45^\circ$ , which excludes any diffusion of the light



Fig. 1. Photograph taken in the French Alps. Emulsion, high-speed infrared; lens focal length =  $55\text{ mm}$ ,  $f/1.2$ ; exposure time, 10 minutes.

from the sun. The phenomenon has been observed at various latitudes, from 25°S in Chile (4) to 70°N in Finland (5), where it can be seen simultaneously with aurorae.

The structures have three size scales. The most typical structures are bands with a separation between bright crests of about 50 km; the bands extend in length over 1000 km. Often more than ten bands are seen from one site. Small-scale structures (on the order of a few kilometers) are detectable. The bands form large clouds, which are difficult to study from a single site. The observing area is limited to a circle with a radius of 1000 km. The maximum size of the large clouds is at least 1000 km.

The main emission in the spectral range used (700 to 890 nm) is due to OH and is concentrated in the infrared. This has been confirmed by spectrophotometric measurements by Peterson (6). However, a contribution from the atmospheric bands of molecular oxygen (761.9 and 864.5 nm) cannot be excluded. The bands are the most striking features of the pictures and we have suggested that they are due to a geometric effect and waves (Fig. 2) (7). It must be noted that the structures are seen only at low angles over the horizon. Photometric measurements as a function of elevation over the horizon are consistent with a layer about 4 km thick and a wave amplitude of 1 km. It is difficult to decide whether these wavy structures are due to interface or gravity waves. However, if observations can be made over a very large area, it will be easier to find correlations between the structures and meteorological perturbations and mountains which can generate gravity waves.

It is difficult to study the large-scale structures from the ground and the horizon is often darkened by haze. From a high-altitude balloon it is possible to avoid tropospheric clouds but the spatial range extends only to 1600 km. A satellite appears the best way to observe the "OH clouds," and the Spacelab 1 flight was a good opportunity. It was not possible on Spacelab 1 to use a photographic camera of the type used on the ground, as the exposure time is too long (of the order of several minutes) and the space shuttle moves at a velocity of 7.8 km sec<sup>-1</sup>. We had the choice of using an image intensified photocamera or a sensitive television camera. Since the shuttle allows recovery of the film, we chose the photocamera, which is a simple instrument, rather than transmitting scientific data by telemetry.

**Instrument.** The main components of the instrument and their operation are

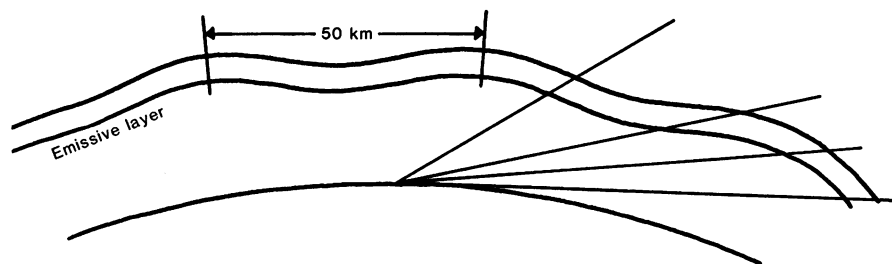


Fig. 2. Geometric effect: variation of the optical path with elevation angle.

briefly as follows. An objective (Angenieux *f*/0.95; focal length, 25 mm) gives an image of the high earth atmosphere on the photocathode of a Thomson micro-channel plate image intensifier. The output of the tube is photographed by an Eclair 16-mm movie camera, which is used frame by frame. Another Angenieux lens is used as a relay lens. All the parts were obtained commercially and were used with only slight modifications for ruggedness: potting for the tube, surface treatment for the gears of the camera, and so on. On one side a mirror projects in front of the relay lens the image from an internal clock; on the other side a similar mirror projects the image from six light-emitting diodes for inflight photometric calibration.

The electronics includes the crystal clock, the command of the stepping motor of the camera, and so on. All the parts are inside a sealed cylinder, which is needed to protect the moisture-sensitive film. Indeed, the space vacuum dries the gelatin and cracks the emulsion. Before flight, the cylinder is filled with dry nitrogen at atmospheric pressure. To avoid water condensation on the optical window, it is made of two disks of glass

separated by a space filled with dry nitrogen. The inner disk is heated by a 0.5-W resistor.

The S20-type photocathode was selected to give maximum sensitivity in the infrared. The maximum gain of the image intensifier is 15,000. It is variable with the incoming light flux by limitation of the high-voltage current. This does not allow absolute photometric measurements but prevents burning of the tube by an excess of light. The experiment was performed to study the morphology of the OH structures. The spectral bandwidth is limited on the short-wavelength end by one of the disks of the optical window, which is made of Schott color glass RG9, and on the long-wavelength end by the photocathode cutoff. The bandwidth (10 percent efficiency) is 700 to 890 nm. The film is a 16-mm black-and-white negative film. The amount of film that can be loaded in the magazine is enough for 4500 pictures.

The instrument was installed on the European pallet perpendicular to the *x* axis and at an angle of 18° with the *y* axis. This tilt angle was used in order to have an image showing part of the sky and a larger part of the earth's atmosphere.

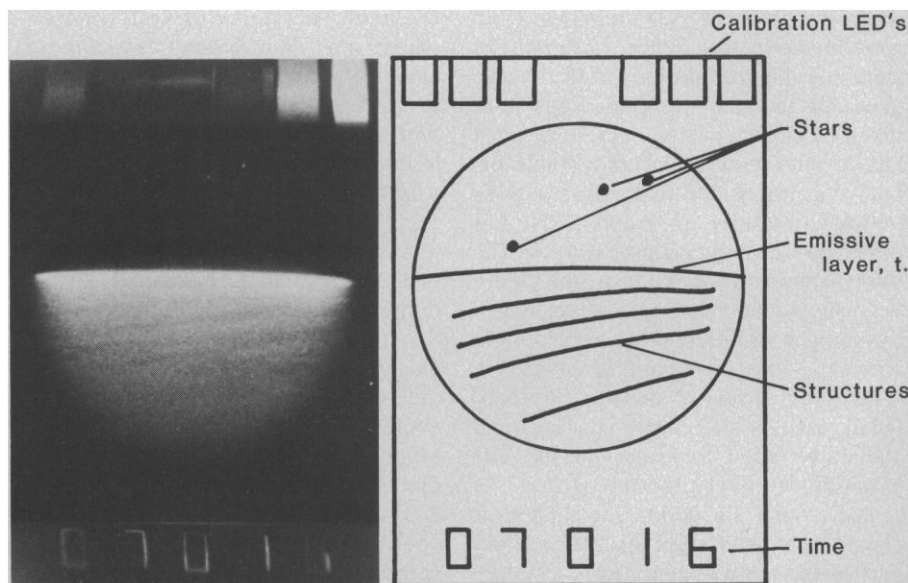


Fig. 3. Picture obtained during the flight. The bright edge is the emissive layer seen tangentially (*t.*).

The instrument works in two modes: in the standby mode, where the internal clock is running and the output for telemetry activated, and in the experiment mode, where the image intensifier is turned on and the camera is working. Several housekeeping parameters are transmitted by telemetry at slow rate: the status of standby and experiment power, image intensifier current, temperature of the film magazine, protective shutter status, day sensor status, temperature status, and stepping motor status (film advance). The scientific data were stored on the film, which is a good medium for information storage. The use of film rather than a television system saved  $10^5$  bits per second when the instrument was operating.

**Flight and preliminary results.** For the flight we chose to take a picture every 16 seconds with alternate exposure times of 0.6 and 1.2 seconds. It was possible to adjust these times by changing straps. The exposure times were expected to be approximately the given ones with the factor of 2 providing some margin. The time between two frames allowed a good overlap of pictures with enough film for the overall flight. The instrument was activated by the Command and Data Management System (CDMS) according to the time line of the experiment. For protection in case of failure of the time line, a light detector would turn off the instrument if the illumination was greater than 2 lux. The crew monitored the temperature and were instructed to turn off the instrument if it was higher than  $40^\circ\text{C}$  (which could destroy the image intensifier) or less than  $-20^\circ\text{C}$  (which could break the film, which is brittle at low temperatures). During the flight the instrument was on during 27 orbits, for a total duration of 528 minutes, and worked perfectly. Extra observations were possible for the study of the shuttle glow. On the whole, 1771 pictures were taken. Unfortunately, the delayed launch date resulted in unfavorable orbits. We expected to make observations between latitudes  $57^\circ\text{S}$  and  $57^\circ\text{N}$ , but coverage was reduced at best  $\pm 35^\circ$ . The observations during the last orbits were very short and the images were fogged by sunlight scattered at the earth's limb. However, the observations covered a total useful surface of about  $2 \times 10^8 \text{ km}^2$  (40 percent of the earth's surface) and should be good for study of the OH structures at low latitudes.

The results are good. Some pictures (Fig. 3) show band-type structures. Only part of the earth appears to be covered by these structures, as we expected from our statistics obtained on the ground.

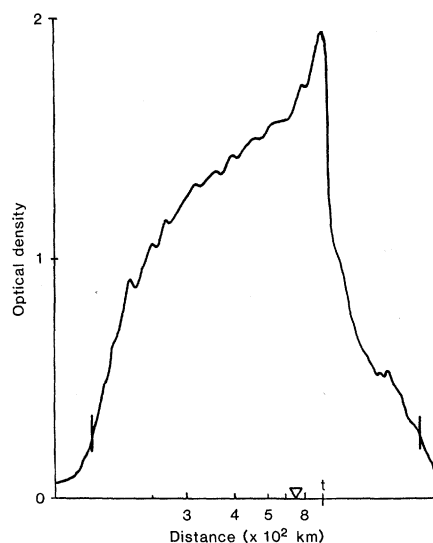


Fig. 4. Microdensitometer tracing along a diameter of Fig. 3. The ordinate is the optical density of the negative. The abscissa is the distance to the subsatellite point at the altitude of 85 km. The triangle indicates the earth's limb.

Figure 4 is a microdensitometer tracing across Fig. 3. We see the strong increase in brightness when the layer is seen tangentially. This increase, due to the larger geometrical optical path, is called the van Rhijn effect. We also see the modulation of the OH wave. In the data processing, classical image processing

will be used to enhance contrast and the structures will be projected in geographic coordinates.

**Conclusion.** The OH emission structures have been observed from space. The shuttle appears to be a perfect platform for our instrument, providing favorable environmental conditions, good flexibility in operation, and the possibility of film recovery. The results will be used to draw a map of the waves near the 85-km level and to attempt to distinguish between interface and gravity waves.

M. HERSÉ

Service d'Aéronomie, Centre National de la Recherche Scientifique, 91370 Verrières-le-Buisson, France

#### References and Notes

1. A. W. Peterson and L. M. Kieffaber, *Nature (London)* **242**, 321 (1973).
2. J. Crawford, P. Rothwell, N. Wells, *ibid.* **257**, 650 (1975).
3. E. B. Armstrong, *J. Atmos. Terr. Phys.* **37**, 1511 (1982).
4. G. Moreels and M. Hersé, *Planet. Space Sci.* **25**, 265 (1977).
5. G. Clairemidi, M. Hersé, G. Moreels, *ibid.*, in press.
6. A. W. Peterson, *Appl. Opt.* **18**, 3390 (1979).
7. M. Hersé, G. Moreels, J. Clairemidi, *ibid.* **19**, 355 (1980).
8. This experiment was supported by the Centre National d'Etudes Spatiales. We thank R. Peyroux for his constant participation in the project and M. Leclere, B. Mege, and A. Vincent for their participation in the development of the instrument. We thank the ESA and NASA teams for their work.

27 March 1984; accepted 23 May 1984

## Observations of Lyman- $\alpha$ Emissions of Hydrogen and Deuterium

**Abstract.** A spectrophotometer was flown on Spacelab 1 to study various mechanisms of Lyman- $\alpha$  emission in the upper atmosphere. The use of absorption cells filled with  $\text{H}_2$  and  $\text{D}_2$  gases allowed us to discriminate a number of weak Lyman- $\alpha$  emissions heretofore masked by the strong H geocoronal emission due to resonance scattering of solar photons. Preliminary results are presented on three topics: the first optical detection of the deuterium Lyman- $\alpha$  emission at 110 kilometers, with an intensity of 330 rayleighs indicating an eddy diffusion coefficient of  $1.3 \times 10^6$  square centimeters per second; auroral proton precipitations seen on both the night and the day side; and an emission located above 250 kilometers of altitude, interpreted as the result of charge exchange of magnetospheric protons with geocoronal atoms.

As part of the European payload complement, a Lyman- $\alpha$  spectrophotometer (experiment 1ES017) was flown on the Spacelab 1 mission in November and December 1983. The observations provide data on atmospheric hydrogen and deuterium atoms, auroral proton precipitations, and a newly observed phenomenon attributed to a "hot" hydrogen emission.

These Lyman- $\alpha$  emissions, whose sources are shown schematically in Fig. 1, can be distinguished from each other by their spectral characteristics. The

most intense emission [intensity  $I_H \sim 20$  kilorayleighs (kR)] comes from the resonance scattering of solar photons by atomic hydrogen in the geocorona at 121.566 nm, which was thoroughly studied by a number of space experiments (1, 2) in the period 1965 to 1972. Therefore, our main objectives with the present Lyman- $\alpha$  spectrophotometer were to observe other sources of Lyman- $\alpha$  emission. The resonance scattering of deuterium atoms at 121.533 nm is well separated from the hydrogen Lyman- $\alpha$  emission at 121.566 nm. Its intensity,  $I_D$ , howev-